Turk J Elec Engin, VOL.8, NO.2 2000, © TÜBİTAK

Radiation from an Impedance Loaded Parallel-Plate Waveguide

Filiz BİRBİR and Alinur BÜYÜKAKSOY
Gebze Institute of Technology, Department of Mathematics,
PO Box 141, Gebze, Kocaeli-TURKEY

Abstract

A hybrid method consisting of employing the mode matching method in conjunction with the Fourier transform technique is used to analyze the radiation of the dominant TEM-wave from an impedance loaded parallel-plate waveguide. The hybrid method that we adopt here reduces the related boundary value problem to a scalar modified Wiener-Hopf equation of the second kind. The solution involves infinitely many unknown constants satisfying an infinite system of linear algebraic equations susceptible to a numerical treatment. Some computational results illustrating the effects of various parameters on the radiation phenomenon are also presented.

1. Introduction

An open-ended waveguide is not normally used as an antenna by itself because of its low directivity. However, waveguides are frequently used as the primary feed to illuminate a paraboloidal reflector, so it is of interest to examine their radiation characteristics. One of the most important open-ended waveguides is the parallel-plate waveguide, which has been subjected to numerous investigations (for example see [1]). In order to secure greater directivity and greater efficiency, generally corrugations are made on the walls of a parallel-plate waveguide. Hence, it is important to investigate the radiation characteristics of a parallel-plate waveguide with corrugations. In this context, Rulf and Hurd [2] investigated the radiation from an open waveguide with reactive walls, which is a canonical model simulating an impedance loaded horn and horn type surface wave launchers. Later, this work was generalized by Büyükaksoy and Birbir [3].

In the present work, the radiation of the dominant TEM mode from a corrugated parallel-plate waveguide shown in Fig. 1a. is analyzed rigorously.

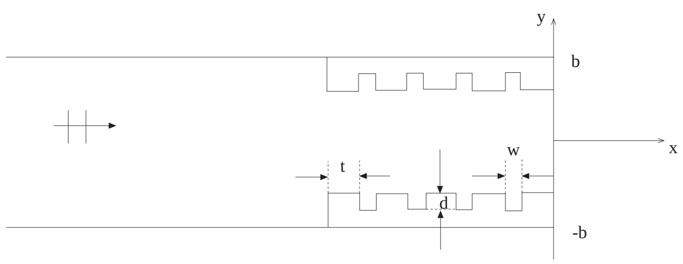

Figure 1a. Geometry of the Parallel-Plate Waveguide with Finite Length of Corrugations

To simplify the analysis, the corrugated surface can be modeled as a constant impedance surface with surface impedance [4]

$$Z = -i\sqrt{\frac{\mu_0}{\epsilon_0}}\frac{w}{w+t}\tan kd, \qquad \frac{w}{w+t} \simeq 1$$

provided that the teeth of the corrugations are vanishingly small. Here w is the width, d is the slot depth and t is the width of the teeth, which are assumed to satisfy the following conditions:

$$w < \lambda/10 \qquad t < w/10$$

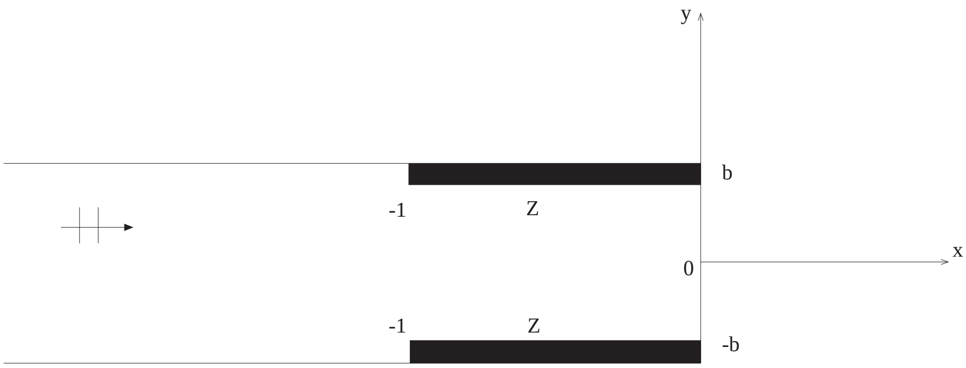

Figure 1b. Equivalent Impedance Loaded Parallel-Plate Waveguide

Hence, the geometry in Fig. 1a is reduced to the configuration shown in Fig. 1b.

By expanding the scattered field into a series of eigen-modes in the waveguide region and using the Fourier transform elsewhere, we get a modified Wiener-Hopf equation of the second kind. The solution involves infinitely many constants satisfying an infinite system of linear algebraic equations. A numerical solution of this system is obtained numerically for various values of the impedance simulating the corrugations and the length of the corrugations wherefrom the effects of these parameters on the radiation phenomenon is studied.

A time factor $e^{-i\omega t}$ with ω being the angular frequency is assumed and suppressed throughout the paper.

2. Analysis

We consider the radiation of the dominant TEM mode from the perfectly conducting parallel plates defined by $S_1 = \{x \in (-\infty, 0), y = b, z \in (-\infty, \infty)\}$, and $S_2 = \{x \in (-\infty, 0), y = -b, \quad z \in (-\infty, \infty)\}$. The parts $x \in (-\ell, 0), y = \pm b \mp 0$ of the inner surfaces of the plates are assumed to be characterized by the same constant surface impedance Z (Fig. 1b). For the sake of mathematical convenience we will assume that the surface impedance is purely reactive, that is, $Z = i\eta Z_0$ with $\eta \in \mathbb{R}$ and Z_0 being the intrinsic impedance of free space. Because of the symmetry with respect to the $x-$axis, we will confine the following analysis to the parallel-plate region formed by an infinite perfectly conducting ground plane $S_0 = \{x \in (-\infty, \infty), y = 0, z \in (-\infty, \infty)\}$ and the half-plane S_1 (Fig. 1c).

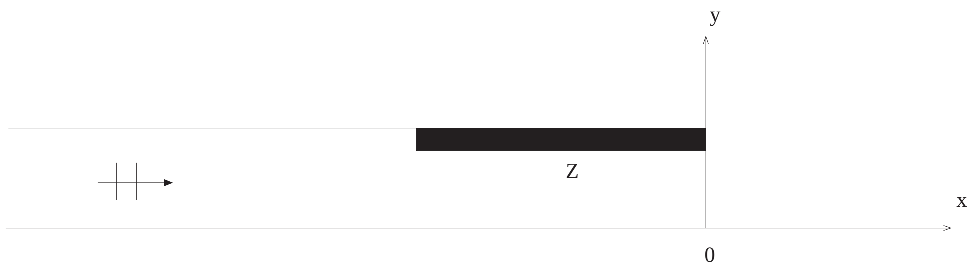

Figure 1c. Problem Equivalent to Figure 1b for Incident Dominant TEM Mode

The configuration is two-dimensional and, with the assumed incident field, only three field components, namely, $H_z = u(x,y)$, $E_x = \frac{i}{\omega\varepsilon_0}\frac{\partial}{\partial y}u(x,y)$ and $E_y = -\frac{i}{\omega\varepsilon_0}\frac{\partial}{\partial x}u(x,y)$, are nonzero.

For analysis purposes, it is convenient to express the total field as follows:

$$u(x,y) = \begin{cases} u_1(x,y), & y > b, \quad x \in (-\infty,\infty) \\ u_2^{(1)}(x,y) + u^i(x,y), & y \in (0,b), \quad x < -\ell \\ u_2^{(2)}(x,y), & y \in (0,b), \quad x \in (-\ell,0) \\ u_2^{(3)}(x,y), & y \in (0,b), \quad x > 0 \end{cases} \tag{1a}$$

Here, u^i is the incident TEM field given by

$$u^i(x,y) = e^{ikx} \tag{1b}$$

with k being the free space wave number.

Total field $u(x,y)$, which satisfies the Helmholtz equation

$$\left(\frac{\partial^2}{\partial x^2} + \frac{\partial^2}{\partial y^2} + k^2\right)u(x,y) = 0, \tag{2}$$

is to be determined with the aid of the following boundary and continuity conditions:

$$\frac{\partial}{\partial y}u_1(x,b) = 0, x < 0 \tag{3a}$$

$$\frac{\partial}{\partial y}u_2^{(1)}(x,b) = 0, x \in (-\infty,-\ell) \tag{3b}$$

$$\frac{\partial}{\partial y}u_2^{(1)}(x,0) = 0, x \in (-\infty,-\ell) \tag{3c}$$

$$\left(\frac{\partial}{\partial y} + k\eta\right)u_2^{(2)}(x,b) = 0, x \in (-\ell,0) \tag{3d}$$

$$\frac{\partial}{\partial y}u_2^{(2)}(x,0) = 0, x \in (-\ell,0) \tag{3e}$$

$$\frac{\partial}{\partial y}u_2^{(3)}(x,0) = 0, x \in (0,\infty) \tag{3f}$$

$$u_1\left(x,b\right)=u_2^{(3)}\left(x,b\right),x>0 \tag{3g}$$

$$\frac{\partial}{\partial y}u_1\left(x,b\right)=\frac{\partial}{\partial y}u_2^{(3)}\left(x,b\right),x>0 \tag{3h}$$

$$u_2^{(1)}\left(-\ell,y\right)+e^{-ikl}=u_2^{(2)}\left(-\ell,y\right), \qquad y\in(0,b) \tag{3i}$$

$$\frac{\partial}{\partial x}u_2^{(1)}\left(-\ell,y\right)+ike^{-ikl}=\frac{\partial}{\partial x}u_2^{(2)}\left(-\ell,y\right), \qquad y\in(0,b) \tag{3j}$$

$$u_2^{(2)}\left(0,y\right)=u_2^{(3)}\left(0,y\right), \qquad y\in(0,b) \tag{3k}$$

$$\frac{\partial}{\partial x}u_2^{(2)}\left(0,y\right)=\frac{\partial}{\partial x}u_2^{(3)}\left(0,y\right), \qquad y\in(0,b) \tag{3l}$$

2.1. The Wiener-Hopf Equation

Since $u_1\left(x,y\right)$ satisfies the Helmholtz equation in the range $x\in(-\infty,\infty)$, its Fourier transform with respect to x gives

$$\left[\frac{d^2}{dy^2}+\left(k^2-\alpha^2\right)\right]F\left(\alpha,y\right)=0 \tag{4a}$$

with

$$F\left(\alpha,y\right)=F_-\left(\alpha,y\right)+F_+\left(\alpha,y\right) \tag{4b}$$

where

$$F_{\pm}(\alpha,y)=\pm\int_0^{\pm\infty}u_1(x,y)e^{i\alpha x}dx \tag{4c}$$

By taking into account the following asymptotic behaviors of u_1 for $x\to\pm\infty$

$$u_1(x,y)=O\left(e^{ik|x|}\right),x\to\pm\infty \tag{5}$$

one can show that $F_+(\alpha,y)$ and $F_-(\alpha,y)$ are regular functions of α in the half planes $\Im m\left(\alpha\right)>\Im m\left(-k\right)$ and $\Im m\left(\alpha\right)<\Im m\left(k\right)$ respectively. The general solution of (4a) satisfying the radiation condition for $y\to\infty$ reads

$$F_-\left(\alpha,y\right)+F_+\left(\alpha,y\right)=A\left(\alpha\right)e^{iK(\alpha)(y-b)} \tag{6}$$

In the Fourier transform, domain (3a) takes the following form

$$\dot{F}_-(\alpha,b)=0 \tag{7}$$

where the $(\cdot)$ specifies the derivative with respect to y. By using the derivative of (6) with respect to y and (7), we get

$$\dot{F}_{+}(\alpha,b)=iK(\alpha)\,A(\alpha)\,. \tag{8}$$

Here, the square root function $K(\alpha)=\sqrt{k^2-\alpha^2}$ is defined in the complex α-plane, cut along $\alpha=k$ to $\alpha=k\infty$ and $\alpha=-k$ to $\alpha=-k\infty$ such that $K(0)=k$.

In the region $0<y<b$ and $x>0$, $u_2^{(3)}(x,y)$ satisfies the Helmholtz equation

$$\left(\frac{\partial^2}{\partial x^2}+\frac{\partial^2}{\partial y^2}+k^2\right)u_2^{(3)}(x,y)=0, x>0 \tag{9}$$

The half-range Fourier transforms of (9) yields

$$\left[\frac{d^2}{dy^2}+K^2(\alpha)\right]G_{+}(\alpha,y)=f(y)-i\alpha g(y) \tag{10a}$$

with

$$f(y)=\frac{\partial}{\partial x}u_2^{(3)}(0,y),\;\; g(y)=u_2^{(3)}(0,y) \tag{10b,c}$$

$G_{+}(\alpha,y)$, which is defined by

$$G_{+}(\alpha,y)=\int_0^\infty u_2^{(3)}(x,y)e^{i\alpha x}dx \tag{11}$$

is a function regular in the half-plane $\Im m(\alpha)>\Im m(-k)$. The general solution of (10a) satisfying (3f) at $y=0$ reads

$$G_{+}(\alpha,y)=D(\alpha)\cos Ky+\frac{1}{K}\int_0^y[f(t)-i\alpha g(t)]\sin K(y-t)\,dt \tag{12}$$

Using (3h), $D(\alpha)$ can be solved uniquely to give

$$D(\alpha)=-\frac{1}{K\sin Kb}\left\{\dot{F}_{+}(\alpha,b)-\int_0^b[f(t)-i\alpha g(t)]\cos K(b-t)\,dt\right\} \tag{13}$$

Replacing (13) into (12) we get

$$G_{+}(\alpha,y)=-\frac{\cos Ky}{K\sin Kb}\left\{\dot{F}_{+}(\alpha,b)-\int_0^b[f(t)-i\alpha g(t)]\cos K(b-t)\,dt\right\}$$

$$+\frac{1}{K}\int_0^y[f(t)-\alpha g(t)]\sin K(y-t)\,dt \tag{14}$$

Although the left-hand side of (14) is regular in the upper half-plane $\Im m\,(\alpha) > \Im m\,(-k)$, the regularity of the right-hand side is violated by the presence of simple poles occurring at the zeros of $K \sin Kb$, namely

$$\alpha_m = \sqrt{k^2 - \left(\frac{m\pi}{b}\right)^2}, m = 0, 1, 2, ... \tag{15}$$

These poles can be eliminated by imposing the condition that their residues are zero. This gives

$$\dot{F}_+\,(\alpha_m, b) = (-1)^m\,\frac{b}{2}\,[f_m - i\alpha_m g_m] \tag{16a}$$

Where K_m, f_m and g_m stand for

$$K_m = K\,(\alpha_m) \tag{16b}$$

$$\left[\begin{array}{c} f_m \\ g_m \end{array}\right] = \frac{2}{b}\int_0^b \left[\begin{array}{c} f\,(t) \\ g\,(t) \end{array}\right] \cos K_m t dt \tag{16c}$$

Consider now the continuity relation (3g) which reads in the Fourier transform domain

$$F_+\,(\alpha, b) = G_+\,(\alpha, b)\,. \tag{17}$$

Taking into account (6), (12) and (17) one obtains

$$\frac{\dot{F}_+\,(\alpha, b)}{K^2 M\,(\alpha)} - F_-\,(\alpha, b) = \frac{1}{K \sin Kb}\int_0^b [f\,(t) - i\alpha g\,(t)] \cos K t dt \tag{18a}$$

with

$$M\,(\alpha) = \frac{\sin Kb}{K} e^{iKb} \tag{18b}$$

Owing to (16c), $f\,(t)$ and $g\,(t)$ can be expanded into cosine series as follows:

$$\left[\begin{array}{c} f\,(t) \\ g\,(t) \end{array}\right] = \sum_{m=0}^{\infty} \frac{1}{p_m} \left[\begin{array}{c} f_m \\ g_m \end{array}\right] \cos K_m t \tag{19a}$$

$$p_m = \left\{\begin{array}{ll} 2, & m = 0 \\ 1, & m \neq 0 \end{array}\right. \tag{19b}$$

Substituting (19a) in (18a) and evaluating the resultant integral, one obtains the following modified Wiener-Hopf equation valid in the strip $\Im m\,(-k) < \Im m\,(\alpha) < \Im m\,(k)$

$$\frac{\dot{F}_+\,(\alpha, b)}{K^2 M\,(\alpha)} - F_-\,(\alpha, b) = -\sum_{m=0}^{\infty} \frac{[f_m - i\alpha g_m]}{p_m} \frac{(-1)^m}{\alpha^2 - \alpha_m^2} \tag{20}$$

The formal solution of (20) can easily be obtained through the classical Wiener-Hopf procedure [5]. The result is

$$\frac{\dot{F}_+\,(\alpha, b)}{(k+\alpha)\,M_+\,(\alpha)} = \sum_{m=0}^{\infty} \frac{[f_m + i\alpha_m g_m]}{p_m} \frac{(-1)^m\,(k+\alpha_m)\,M_+\,(\alpha_m)}{2\alpha_m\,(\alpha+\alpha_m)} \tag{21}$$

Here, $M_+(\alpha)$ is the split function, regular and free of zeros in the upper half-plane $\Im m(\alpha) > \Im m(-k)$, resulting from the Wiener-Hopf factorization of the functions $M(\alpha)$ as

$$M(\alpha) = M_+(\alpha) M_-(\alpha), \qquad M_-(\alpha) = M_+(-\alpha) \tag{22a,b}$$

The explicit expressions of $M_+(\alpha)$ is given in [5] as follows:

$$M_+(\alpha) = \sqrt{\frac{\sin kb}{k}} \exp\left\{\frac{ibK}{\pi} \ln\left(\frac{\alpha + K}{k}\right)\right\}$$

$$\times \exp\left\{\frac{ib\alpha}{\pi}\left(1 - \mathcal{C} + \ln\left(\frac{2\pi}{kb}\right) + i\frac{\pi}{2}\right)\right\} \prod_{m=0}^{\infty}\left(1 + \frac{\alpha}{\alpha_m}\right) e^{\frac{i\alpha b}{m\pi}} \tag{23}$$

where $\mathcal{C}$ is Euler's constant given by $\mathcal{C}$=0.57721....

2.2. Determination of the Constants f_m and g_m

Consider now the waveguide region $y \in (0, b), x < 0$. By using the boundary conditions in (3b,c) the scattered field $u_2^{(1)}(x, y)$ can be expressed in terms of normal modes as follows:

$$u_2^{(1)}(x, y) = \sum_{n=0}^{\infty} \frac{a_n}{p_n} e^{-i\alpha_n x} \cos K_n y \tag{24}$$

Similarly, the series expansion of $u_2^{(2)}(x, y)$ in the region $y \in (0, b), x \in (-\ell, 0)$ can be obtained by taking into account the boundary conditions in (3d,e). The result is

$$u_2^{(2)}(x, y) = \sum_{n=0}^{\infty} \left[b_n e^{i\beta_n x} + c_n e^{-i\beta_n x}\right] \cos \gamma_n y \tag{25a}$$

where $\pm\beta_n$ are the symmetrical roots of the characteristic equation

$$L(\pm\beta_n) = 0, \tag{25b}$$

with

$$L(\alpha) = K \sin Kb - k\eta \cos Kb, \tag{25c}$$

and

$$\gamma_n = K(\beta_n). \tag{25d}$$

Note that the solution of the Wiener-Hopf equation in (21) involves two sets of unknown constants, f_m and g_m. In order to determine these constants, consider finally the continuity relations (3i-l) with (10b,c). From these relations, using (24), (25a) and (19b), one obtains

$$\sum_{n=0}^{\infty} \left[b_n e^{-i\beta_n \ell} + c_n e^{i\beta_n \ell}\right] \cos \gamma_n y = \sum_{m=0}^{\infty} a_m e^{i\alpha_m \ell} \cos K_m y + e^{-ikl} \tag{26a}$$

$$-\sum_{n=0}^{\infty} i\beta_n \left[b_n e^{-i\beta_n \ell} - c_n e^{i\beta_n \ell}\right] \cos\gamma_n y = \sum_{m=0}^{\infty} i\alpha_m a_m e^{i\alpha_m \ell} \cos K_m y + ike^{-ikl} \tag{26b}$$

$$\sum_{n=0}^{\infty} [b_n + c_n] \cos\gamma_n y = \sum_{m=0}^{\infty} \frac{g_m}{p_m} \cos K_m y \tag{26c}$$

$$\sum_{n=0}^{\infty} i\beta_n [b_n - c_n] \cos\gamma_n y = \sum_{m=0}^{\infty} \frac{f_m}{p_m} \cos K_m y \tag{26d}$$

$$q_n = \frac{b}{2}\left[1 + \frac{\sin^2\gamma_n b}{k\eta b}\right] \tag{26e}$$

Let us multiply both sides of (26a,d) by $\cos\gamma_n y, n = 0, 1, 2, ...$ and integrate from $y = 0$ to $y = b$ to get

$$q_n \left[b_n e^{-i\beta_n \ell} + c_n e^{i\beta_n \ell}\right] = \sum_{m=0}^{\infty} a_m e^{i\alpha_m \ell} \frac{(-1)^m \gamma_n}{\gamma_n^2 - K_m^2} \sin\gamma_n b + e^{-ikl} \frac{\sin\gamma_n b}{\gamma_n} \tag{27a}$$

$$\beta_n q_n \left[b_n e^{-i\beta_n \ell} - c_n e^{i\beta_n \ell}\right] = -\sum_{m=0}^{\infty} \alpha_m a_m e^{i\alpha_m \ell} \frac{(-1)^m \gamma_n}{\gamma_n^2 - K_m^2} \sin\gamma_n b + ke^{-ikl} \frac{\sin\gamma_n b}{\gamma_n} \tag{27b}$$

$$q_n [b_n + c_n] = \gamma_n \sin\gamma_n b \sum_{m=0}^{\infty} \frac{g_m}{p_m} \frac{(-1)^m}{\gamma_n^2 - K_m^2} \tag{27c}$$

$$i\beta_n q_n [b_n - c_n] = \gamma_n \sin\gamma_n b \sum_{m=0}^{\infty} \frac{f_m}{p_m} \frac{(-1)^m}{\gamma_n^2 - K_m^2}. \tag{27d}$$

The elimination of b_m and c_m between (27a,d) yields

$$\sum_{m=0}^{\infty} \frac{[f_m + i\beta_n g_m]}{ip_m} \frac{(-1)^m}{\gamma_n^2 - K_m^2} = -\sum_{m=0}^{\infty} a_m e^{i(\alpha_m + \beta_n)\ell} \frac{(-1)^m}{\beta_n + \alpha_m} - \frac{e^{i(\beta_n - k)l}}{\beta_n - k} \quad n = 0, 1, 2, 3, ... \tag{28a}$$

$$e^{i\beta_n l} \sum_{m=0}^{\infty} \frac{[f_m - i\beta_n g_m]}{ip_m} \frac{(-1)^m}{\gamma_n^2 - K_m^2} = -\sum_{m=0}^{\infty} a_m e^{i\alpha_m \ell} \frac{(-1)^m}{\beta_n - \alpha_m} - \frac{e^{-ikl}}{\beta_n + k} \quad n = 0, 1, 2, 3, ... \tag{28b}$$

On the other hand, by substituting $\alpha = \alpha_n$ in (21) and using (16a), we obtain the following result:

$$\frac{b}{2} \frac{(-1)^n [f_n - i\alpha_n g_n]}{(k + \alpha_n) M_+(\alpha_n)} = \sum_{m=0}^{\infty} \frac{[f_m + i\alpha_m g_m]}{2\alpha_m (\alpha_n + \alpha_m)} \frac{(-1)^m (k + \alpha_m) M_+(\alpha_m)}{p_m} \quad n = 0, 1, 2, 3, ... \tag{29}$$

The unknown constants f_n, g_n and a_n can now be determined by solving (29) together with (28a,b). This infinite system of linear algebraic equations is solved approximately by truncating the expansion series. In the numerical results, the truncation number N of n is taken as $N = 10$.

3. Analysis of The Field

The radiated field in the region $y > b$ can be obtained by taking the inverse Fourier transform of $F(\alpha, y)$. By using (8) we write

$$u_1(x, y) = \frac{1}{2\pi} \int_{\mathcal{L}} \frac{\dot{F}_+(\alpha, b)}{iK(\alpha)} e^{iK(\alpha)(y-b)} e^{-i\alpha x} d\alpha \tag{30}$$

where $\mathcal{L}$ is a straight line parallel to the real axis lying in the strip $\Im m(-k) < \Im m(\alpha) < \Im m(k)$. The asymptotic evaluation of the integral in (30) through the saddle point technique yields for the radiated field

$$u_1(x, y) = -\frac{e^{i\pi/4}}{\sqrt{2\pi}} \dot{F}_+(-k\cos\phi, b) \frac{e^{ik\rho}}{\sqrt{k\rho}} \tag{31a}$$

which can also be written as

$$u_1(x, y) = -\frac{e^{i\pi/4}}{\sqrt{2\pi}} \sum_{m=0}^{\infty} (-1)^m \frac{[f_m + i\alpha_m g_m]}{p_m} \frac{(k+\alpha_m)(k - k\cos\phi) M_+(\alpha_m) M_+(-k\cos\phi)}{2\alpha_m(\alpha_m - k\cos\phi)} \frac{e^{ik\rho}}{\sqrt{k\rho}} \tag{31b}$$

where Eq. (21) has been taken into account. In the above expressions, (ρ, ϕ) stands for the cylindrical polar coordinates defined by

$$x = \rho\cos\phi, \;\; y - b = \rho\sin\phi. \tag{31c}$$

4. Numerical Results

In this section, some graphics displaying the results obtained in this paper and showing the effects of various parameters such as the waveguide width, the corrugation length and the impedance simulating the corrugation on the radiation phenomenon are presented.

Fig. 2a and Fig. 2b show the effect of the impedance on the radiated field for $b < \lambda/2$ and $b > \lambda/2$, respectively. In the first case, only the dominant TEM mode is present in the corrugated region, while in the second case, in addition to the TEM mode, the TE_{01} mode is also excited. It is observed that for negative values of the reactance the directivity increases, i.e., the main beam becomes narrower with increasing values of $|\eta|$. However, one should note that over a certain reactance value, the side lobe also becomes significant (see Fig. 2b).

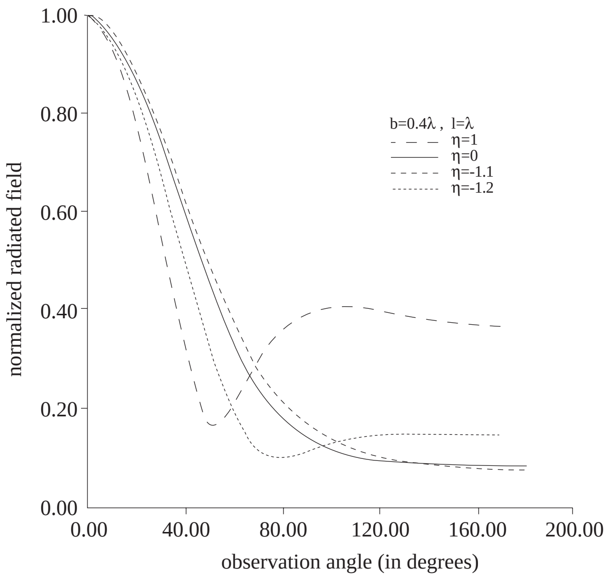

Figure 2a. Radiated field for $b < \lambda/2$ versus observation angle

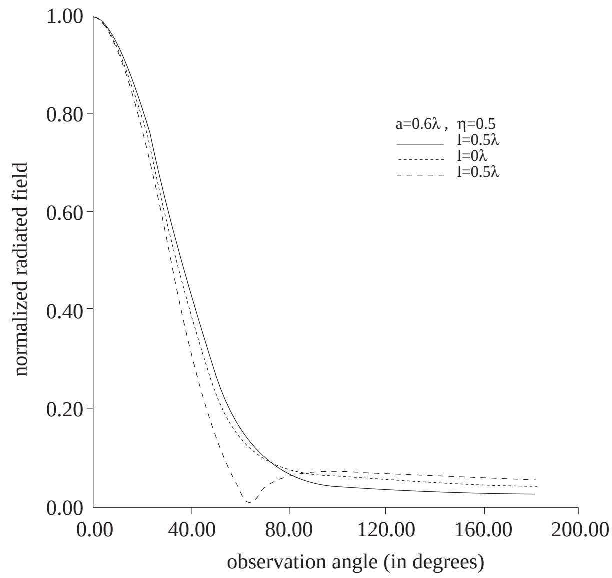

Figure 2b. Radiated field for $b > \lambda/2$ versus observation angle

Fig. 3a and Fig. 3b depict the effects of the corrugation length on the radiated field for $\eta > 0$ and $\eta < 0$, respectively. It is observed that the length of the corrugation affects the radiation pattern. Indeed, for $\eta > 0$ the directivity can be increased by increasing ℓ. For $\eta < 0$ the same effect is observed but in this case the side lobes become important.

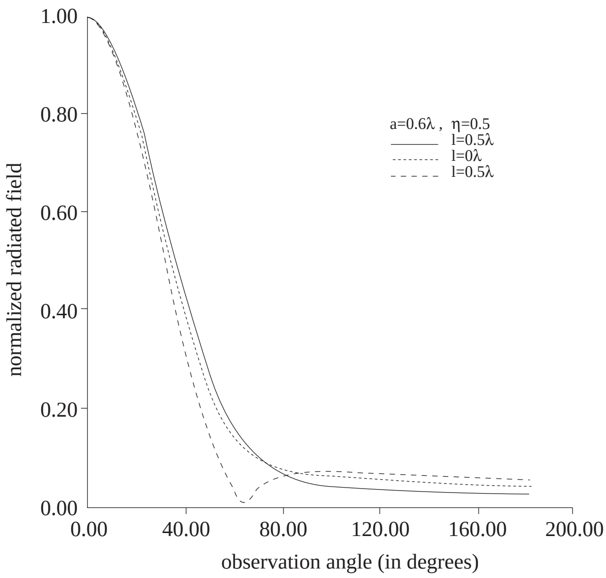

Figure 3a. Radiated field for $\eta > 0$ versus observation angle

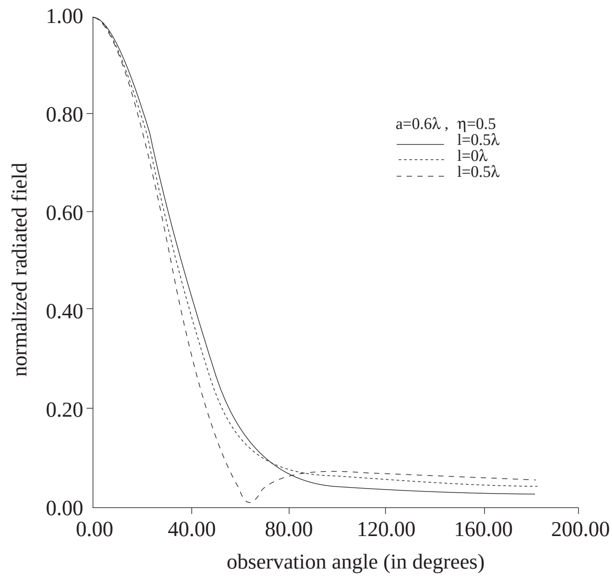

Figure 3b. Radiated field for $\eta < 0$ versus observation angle

5. Concluding Remarks

In this work a rigorous analysis is carried out to obtain the radiation characteristics of a parallel-plate waveguide with finite corrugations. By simulating the corrugations by a constant surface reactance, the boundary value problem is formulated as a modified Wiener-Hopf equation involving three sets of unknowns satisfying three infinite systems of linear algebraic equations. These equations are solved numerically and some computational results showing the effects of the reactance simulating the corrugations and the corrugation length on the radiation pattern are presented. It can be easily checked that for $\eta = 0$, the results obtained in this work reduce those related to the perfectly conducting parallel-plate waveguide.

References

[1] L.A. Weinstein, "The Theory of Diffraction and the Factorization Method," The Golem Press, Boulder, Colorado, 1967

[2] B. Rulf and R.A. Hurd, "Radiation from an open waveguide with reactive walls," IEEE Trans. Antennas and Propagat., Vol.AP-26, No.5, 1978

[3] A. Büyükaksoy and F. Birbir, "Analysis of an Impedance Loaded Parallel-Plate Waveguide Radiator," Journal of Elecetromagnetic Waves and Applications, Vol.12, 1509-1526, 1998

[4] R.S. Elliot, "On the Theory of Corrugated Plane Surfaces," IRE Trans. Antennas and Propagat. Vol. AP-12, 71-81, 1954

[5] R. Mittra and S.W. Lee, *Analytical Techniques in the Theory of Guided Waves*, The Macmillan Company, New York, 1971